Available online at www.sciencedirect.com
SCIENCE DIRECT
Journal of Photochemistry and Photobiology A: Chemistry 181 (2006) 363–369
Journal of Photochemistry and Photobiology A:Chemistry
www.elsevier.com/locate/jphotochem

Performance and characterization of Ag–cotton and Ag/TiO_2 loaded textiles during the abatement of *E. coli*

T. Yuranova [a], A.G. Rincon [b], C. Pulgarin [b], D. Laub [c], N. Xantopoulos [d], H.-J. Mathieu [d], J. Kiwi [a,*]

[a] *Laboratory of Photonics and Interfaces, Institute of Chemical Sciences and Engineering, Station 6, Lausanne, Switzerland*
[b] *Institute of Chemical Sciences and Engineering, Group of Electrochemical Engineering, Station 6, Lausanne, Switzerland*
[c] *Interdisciplinary Center for Electron Microscopy (CIME), Lausanne, Switzerland*
[d] *Laboratory of Metallurgical Engineering, Materials Department, Swiss Federal Institute of Technology, 1015 Lausanne, Switzerland*

Received 22 July 2005; received in revised form 2 December 2005; accepted 19 December 2005
Available online 19 January 2006

Abstract

The bacterial inactivation of *Escherichia coli* on Ag–cotton textiles were investigated under different experimental conditions with novel Ag-nanoparticles fixed on cotton textiles. The evaluation of the bactericide performance of the Ag–cotton was compared with the one observed for Ag–TiO_2–cotton loaded textiles. The procedure used allowed us to prepare highly dispersed Ag-cluster species, 2–4 nm in size, as observed by transmission electron microscopy (TEM). By depth profile analysis, the X-ray photoelectron spectroscopy (XPS) revealed that the Ag profile in the 15 topmost layers remained almost constant before and after *E. coli* inactivation. The cotton loading was fairly low and of the order of 0.10 wt.% Ag/wt. of cotton. By infrared spectroscopy no modification of the Ag–cotton could be detected before or after *E. coli* inactivation due to the small absorption coefficient of Ag and the very low metal loading of Ag on the cotton. The *E. coli* was completely abated on Ag–cotton textiles immediately after the contact took place, due to the strong bacteriostatic effect of the dispersed silver clusters on the cotton surface.

Keywords: Ag-clusters; *E. coli* decontamination; XPS; IR; Ag–cotton textiles

1. Introduction

Silver solutions and silver clusters have been used for the treatment of infections due to their natural bactericide and fungicide properties [1–4]. Nano-silver particles in solution or supported on appropriate substrates are currently used due to their effective action adversely affecting the cellular metabolism and inhibiting cell growth. The chemistry has revealed that an Ag-deposit is not toxic to human cells in vivo and is reported to be biocompatible [5–8]. Previous work report that Ag as hinders the transport of vital cations in the pores of the microbial cell membranes, affecting the electron transfer system necessary for the basic bacterial metabolism [9–11]. Moreover, it was reported that Ag does not introduce any of the delivery problems encountered with anti-bacterial drugs [12].

Ag-salts and silver solutions have some biological limitations for their practical use as a bactericide. Supported silver clusters prepared using nano-technology seem promising when fixed on adequate supports due to their increased bactericide effect. This is important in wound healing and for the control of inflammations. By decreasing the Ag crystal size the dispersion of the clusters and the active Ag contact area available for chemical reactions is increased. This in turn allows the reactions to proceed over a short time period.

This study investigated the fixation of Ag on cotton (from now on cotton–Ag) that would protect wounds from bacterial contamination and growth. The bacteria existing in the wound exudates in contact with the cotton–Ag, which inhibits the growth and multiplication of bacteria, *Escherichia coli* K-12 taken as a model for this study [13]. Some runs were also tried for Ag–TiO_2 cotton systems to see whether this system under band-gap light irradiation would have a more effective bactericide action on *E. coli* than Ag–cotton alone. Studies of this system in suspensions have been reported [14–16]. Recently the Ag-fixation on healing

* Corresponding author.
E-mail address: john.kiwi@epfl.ch (J. Kiwi).

1010-6030/$ – see front matter © 2005 Elsevier B.V. All rights reserved.
doi:10.1016/j.jphotochem.2005.12.020

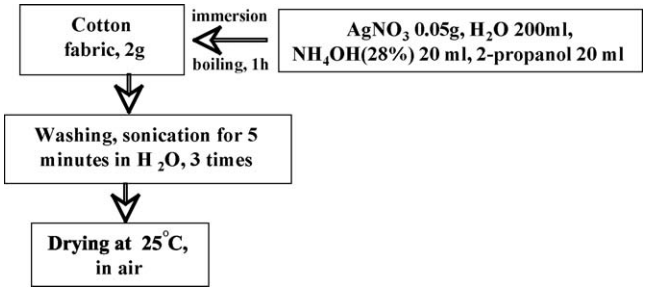

Fig. 1. Schematic of the preparation of the Ag-loaded cotton textiles.

pads by modifying the textile surfaces before the Ag deposition has been reported [17]. During this study we performed a long series of preliminary experiments to find the most suitable conditions in order to attach Ag-clusters on the cotton textile. The bactericide performance of the Ag–cotton was evaluated. Finally, we proceeded to characterize the Ag-clusters on the cotton by electron microscopy (EM), photoelectron spectroscopy (XPS) and infrared spectroscopy (IR).

2. Experimental

2.1. Materials

Reagents like $AgNO_3$, ammonia solution, isopropanol, acid and bases were Fluka p.a. and used without further purification.

2.2. Fixation of silver on cotton textiles

Fig. 1 shows schematically the procedure used to fix the Ag-clusters on the cotton textile. The precursor solution was prepared by adding isopropanol to the ammonia aqueous solution of $AgNO_3$. The cotton textile was then immersed in this solution and boiled for 1 h. Subsequently, the Ag–cotton sample was removed from the solution, washed with water and sonicated several times before drying at 25 °C [18]. This procedure led to loadings of around 0.1 wt.% Ag/wt. cotton as determined by elemental analysis.

The TiO_2 loaded cotton was prepared by immersing the cotton textile sample in a 5 g/l suspension of TiO_2 Degussa P-25, previously sonicated for 30 min in bi-distilled water. The textile was then dried for 1 h and sonicated for 5 min at 75 °C to eliminate loosely bound particles. The loading of the cotton was around 1% TiO_2/wt. on cotton as determined by elemental analysis. When Ag-clusters were added on top of the TiO_2 on the cotton, the Ag-clusters were fixed as described in the preceding paragraph.

2.3. Bacterial strain quantification

The bacterial strain used *Escherichia coli* K12 was inoculated in the nutrient broth no. 2 (N. Oxoid 2, Switzerland) and grown overnight at 37 °C by constant agitation under aerobic conditions. Aliquots of the overnight culture were inoculated into a fresh medium and incubated aerobically at 37 °C for 15 h. At a stationary growth phase, bacteria cells were collected by centrifugation at $500 \times g$ for 10 min at 4 °C and the bacterial pellets were washed three times with a tryptone solution. Cell suspensions were diluted with Milli-Q water in a glass bottle to the required cell density corresponding to 10^5 to 10^6 colony forming units per millilitre (CFU/ml). Samples were spotted onto plates and spread using standard techniques. Samples were plated on agar PCA (Plate Count Agar) plates. The plates were incubated at 37 °C for 24 h for the final bacterial counting. The experimental results reported for *E. coli* inactivation in Fig. 6a–e are the media of four independent runs.

2.4. Photocatalysis experiments with the system Ag–TiO_2–cotton

At the beginning of the experiments while reactors were kept in the dark (5 min), bacteria were added to a glass bottle and mixed by recirculation of the water to constant concentration throughout the system. All experiments were carried out with Milli-Q water. Then the solar lamp was turned on at an intensity of 100 mW/cm^2 and samples were collected at predetermined times for 3 or 4 h. All experiments were repeated three times and the weighted average was taken to report the data in Fig. 6d to 6e. Samples were also collected at predetermined times (t) in the dark (controls). The experiments were carried out under artificial light using thin film Pyrex glass reactors with an illuminated volume of 25 ml. A peristaltic pump recirculated the water from the recirculation tank to the reactors with a flow rate of 150 ml/min. The total volume of the system (100 ml) is made up by the 25 ml irradiated volume and the dead volume (recirculation tank + connecting tubing). Internal PVC supports were put in the reactors to carry out the irradiation of the bleached cotton with fixed Ag–TiO_2. The solar simulated Xe-lamp (Suntest, Her-

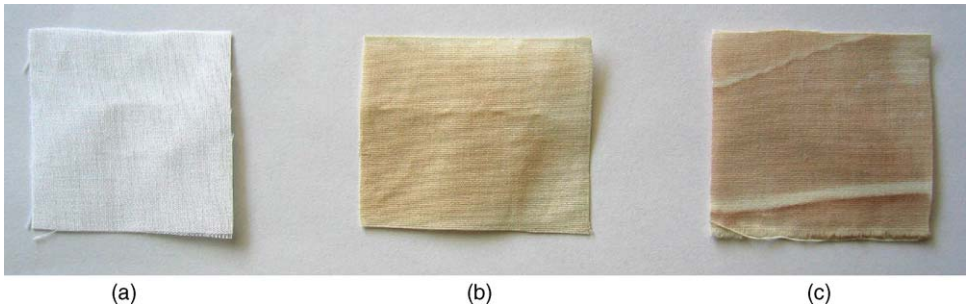

Fig. 2. Cotton pads before Ag-loading (a), after Ag-loading but before being used in *E. coli* inactivation (b) and after their use in *E coli* inactivation (c).

aeus, Hanau, Germany) has a light spectral distribution of about 0.5% of the emitted photons at wavelengths <300 nm and about 6% between 300 and 400 nm. The emission spectrum between 400 and 800 nm follows the solar spectrum.

2.5. Transmission electron microscopy (TEM)

A Philips EM 430 (300 kV, LaB_6, 0.23 nm resolution) equipped with an energy dispersive spectrometer (EDS) was used to measure the particles sizes of the Ag-clusters on the cotton fabrics. The textiles were embedded in epoxy-resin (EPON 812) and polymerized at 60 °C. The fabrics were cross-sectioned with an ultra-microtome (Ultracut E, Reichert-Jung) to thin sections of 50–70 nm at room temperature. Magnification from about 1000× up to 450 000× was used to characterize the samples. In this way, it was possible to provide overview images up to images with resolution up to 0.5 nm as shown in Fig. 3b. The instrument used for electron microscopy was equipped with an energy dispersive X-ray analysis EDAX to identify the deposition of Ag-clusters on the textile fabric.

2.6. X-ray photoelectron spectroscopy (XPS)

Measurements were carried out in a Kratos Axis Ultra instrument equipped with a conventional hemispheric analyzer. The X-ray source employed was an Al Kα 1486.6 eV operated at 150 W and UHV 10^{-9} mbar. The analysis area was 100 μm at an angle of 90° relative to the substrate surface. The pass energies were 80 and 20 eV for wide scans and high resolution elemental scans, respectively. The operating software used was Vision 2 which corrects for the transmission function. Charge compensation was performed with a self-compensating device (Kratos patent) using field emitted low energy electrons (0.1 eV) to adjust the main C–C component to 285 eV. Sputtering was performed by Ar-ions applying a primary beam energy of 2 kV.

2.7. Elemental analysis

Elemental analysis of the Ag loaded cotton was carried out by atomic absorption spectrometry using a Perkin-Elmer 300 S unit.

2.8. X-ray diffraction measurements (XRD) of TiO_2 loaded textiles

The crystallinity of the Ag-clusters on the cotton surface was studied with a Siemens X-ray diffractometer using Cu Kα radiation. However, not enough signals were obtained to characterize the Ag crystallites due to the small size and low loading attained on the cotton textile.

2.9. Attenuated total reflection infrared (ATR-IR) spectroscopy

The ATR-IR spectra were measured in a Portman Instrument AG spectrophotometer equipped with a Specac attachment (45° one pass diamond crystal). The spectra obtained were the results of 256 scans with a 0.5 cm^{-1} resolution in the spectral range of the infrared spectrophotometer between 2000 and 800 cm^{-1}.

3. Results and discussion

3.1. Deposition of the Ag-clusters on cotton textiles

Fig. 2 shows the cotton pads used in the bacterial and in the control experiments. From left to right: pads before Ag-loading, after silver loading but before contact with the solution

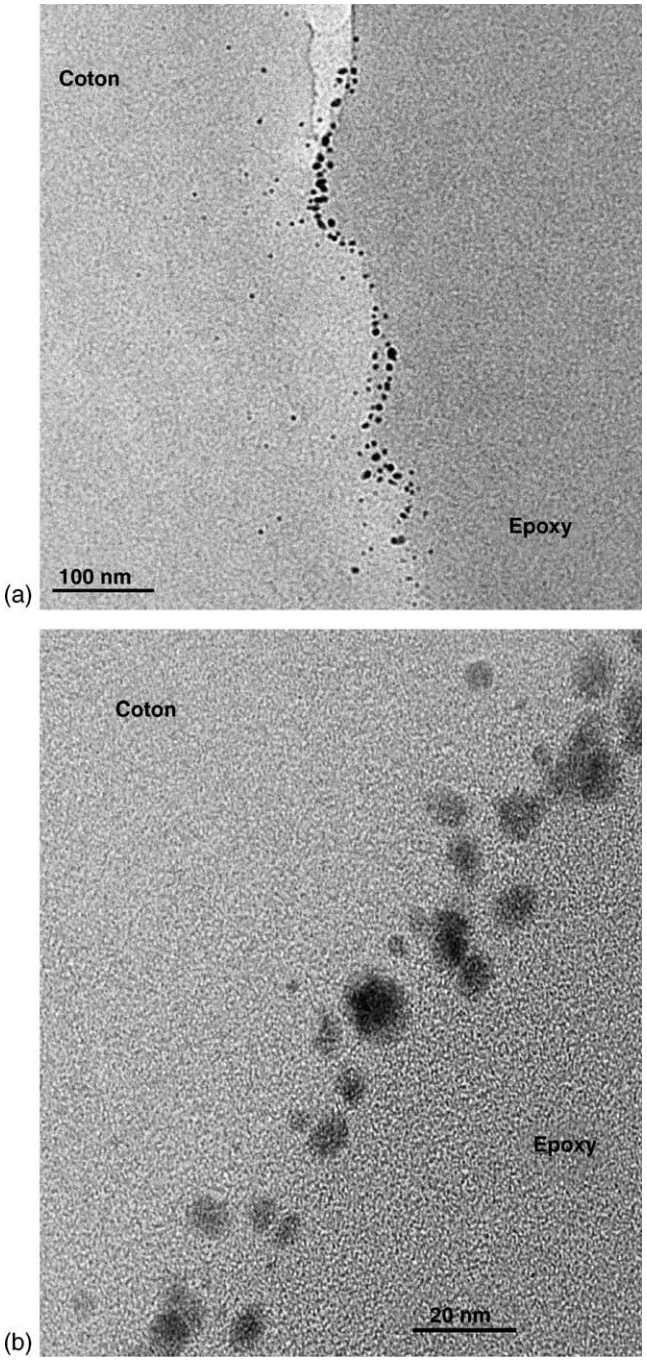

Fig. 3. (a) TEM of the Ag-clusters on the cotton textile deposited as described in the experimental section. (b) High-magnification TEM of the Ag-clusters on the cotton showing the dimensions of the Ag-clusters. For other details see text.

containing *E. coli* and after *E. coli* inactivation. The brownish color of the Ag-nanoparticles on the cotton absorbs light of different wavelengths and a characteristic broad absorption band appears in the visible range. The Ag-clusters which produce the brownish color during the reduction of the Ag^+-ions of the Ag-nitrate by isopropanol, agglomerate rapidly and grow during the Ag-loading of the cotton. Recent work confirmed that the intermediate complex of $Ag(NH_3)_2{}^+$-ions is reduced by ethanol and isopropanol [1,7]. The dark gray-brown color is observed in the pad shown in Fig. 2c (right-hand side of Fig. 2) after the abatement of *E. coli*. The Ag-clusters deposited on the surface (see Section 2) easily enter the core of the cotton textile after their immersion in the *E. coli* aqueous solution and encounter reducing sacrificial species in the cellulose that makes up the cotton. This accounts for the growth of the Ag-clusters leading to the formation of larger metallic Ag nano-particles (see Eq. (1)) besides the reduction of some Ag-ionic species in the solution remaining from the $Ag(NH_3)_2{}^+$-ions present in the preparation of the Ag-clusters (see Fig. 1):

$$Ag_m{}^+ + e^- \rightarrow Ag_m \quad (1)$$

The amount of Ag found by elemental analysis was 0.10 wt.% Ag/wt. cotton textile at time zero and the same after the abatement of the *E. coli* (see Fig. 6c below).

3.2. Transmission electron microscopy (TEM) of the Ag-particles on cotton

Fig. 3a shows the Ag-clusters on the cotton textiles and also in the topmost layers where they have penetrated by diffusion. Fig. 3a has been obtained after the cotton sample has been cross-sectioned with an ultra-microtome. A view with a higher magnification of the Ag-particles is presented in Fig. 3b. The state of the Ag in the particle sizes 2–12 nm was not characterized since it was beyond the experimental scope of the facilities

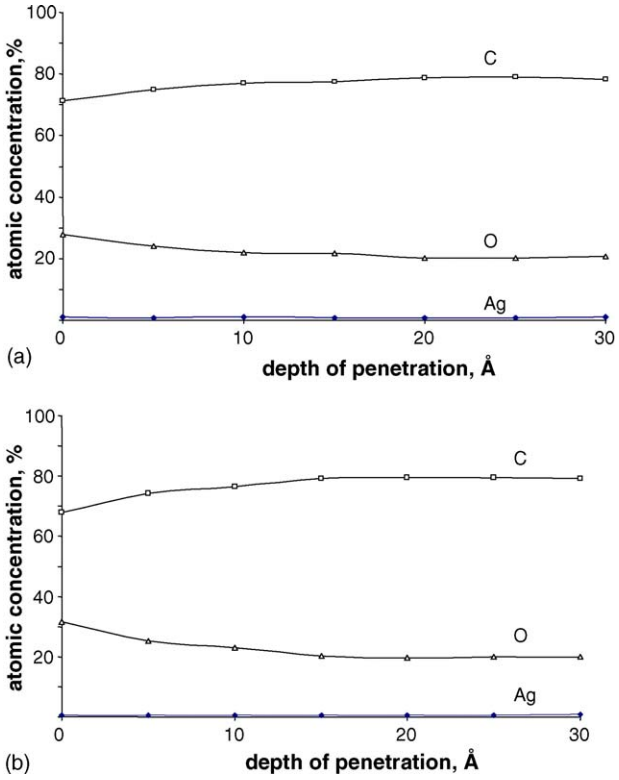

Fig. 4. XPS depth profile of Ag–cotton samples used in the dark before and after *E coli* complete inactivation as shown in Fig. 6c.

available in this study. In the particles shown in Fig. 3b, silver was detected. But these silver particles could be in the form of crystallites, composite thin particles bound to the cellulose units of the cotton or highly dispersed Ag-crystallites. The brownish color of the Ag–cotton presented in Fig. 2b and c confirmed the presence of Ag^0. But the presence of Ag_2O and AgO cannot be excluded as reported for silver loaded textiles [17]. The clusters in Fig. 3b and the color of the loaded Ag–cotton reported

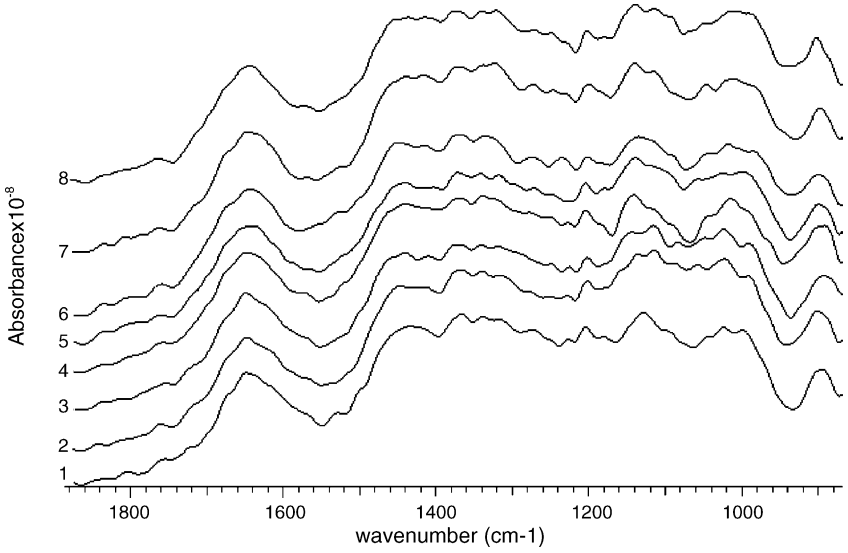

Fig. 5. ATR-IR spectroscopy of cotton and Ag–cotton samples: (1) Cotton alone, (2) Ag–cotton before use, (3) Ag–cotton sample after *E. coli* abatement in the dark, (4) Ag–cotton sample after *E. coli* abatement under light, (5) TiO_2–cotton before use, (6) TiO_2–cotton before use and after 4 h suntest irradiation, (7) Ag–TiO_2–cotton before use, (8) Ag–TiO_2–cotton after 4 h Suntest irradiation.

in Fig. 2 suggests that Ag^0-clusters exist on the textile surface. These uncharged clusters, by contact and minimal dissolution of Ag or Ag-ionic forms, have been reported to be responsible for the abatement of *E. coli* and other biological effects [3–12].

3.3. X-ray photoelectron spectroscopy of Ag–cotton surfaces

Fig. 4 presents the atomic concentration percentage of the cotton by the Ag, O and C as a function of the depth of penetration of the Ar-ions (profile depth). It is readily seen that the amounts of O, Ag and C stay almost the same up to 30 Å. This is an equivalent depth of about 15 layers. The depth profile experiments were carried out for several minutes and the rate of penetration of the textile layers were referenced with the known rate of tantalum (Ta) of 15 atomic layer/min or around 30 Å [19]. The surface atomic concentration is seen to remain stable before and after the catalytic runs (Fig. 4). The Ag 3d doublet was analyzed in terms of the Ag^0, Ag^+ and Ag^{2+} components. The deconvolution of the XPS signals by Gaussian–Lorentzian

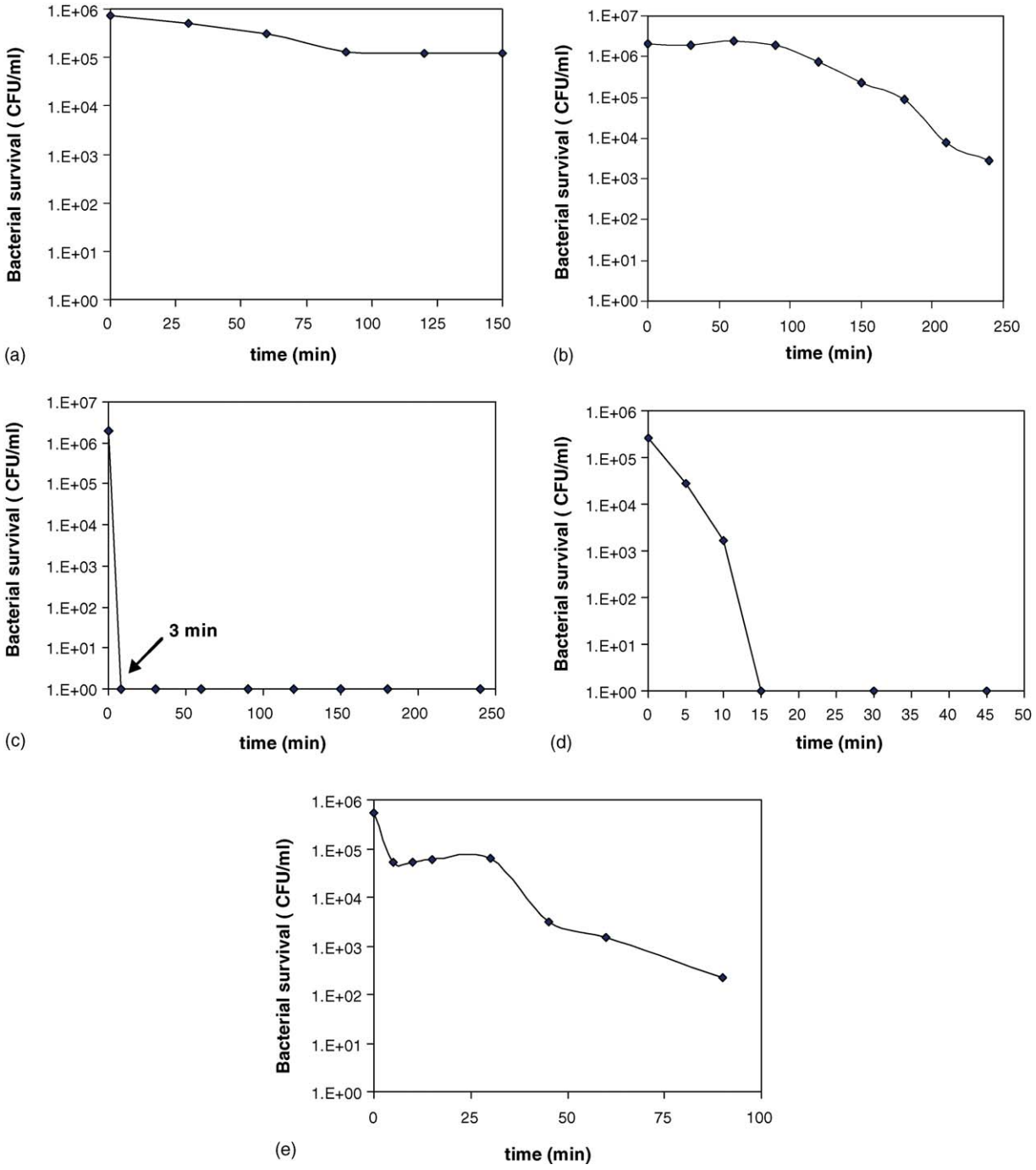

Fig. 6. (a) *E. coli* bacterial survival on cotton alone in the dark, (b) *E. coli* bacterial survival on cotton alone under Suntest solar simulated light (100 mW/cm^2), (c) *E. coli* bacterial survival on Ag–cotton samples in the dark, (d) *E. coli* bacterial survival on Ag–TiO_2–cotton samples in the dark, (e) *E. coli* bacterial survival on Ag–TiO_2–cotton samples under light.

curve fitting was not possible. The peak positions of 368.2 eV for Ag^0, 367.8 eV for Ag^+ and 367.4 eV for Ag^{2+} were taken as reference values to resolve the XPS peaks [19].

3.4. Infrared spectroscopy of Ag–cotton samples

Fig. 5 presents the ATR–FT-IR spectra of eight different samples of cotton and Ag–cotton samples under different preparation conditions and use. The spectral details are described in the captions to Fig. 5. The spectral profiles are conserved under the different experimental conditions used and do not allow more detailed analysis of any changes of the Ag-clusters. The main evidence by the ATR-IR experiments in Fig. 5 is that the small clusters of Ag formed do not modify the cotton surface. Also, the small amount of (Ag 0.10%) and the fact that the Ag-clusters have very small absorption coefficients makes them difficult to detect by IR-spectroscopy.

3.5. The performance of Ag–TiO_2–cotton during bactericide applications

Fig. 6a–d presents the experimental results for the bacteriostatic action of Ag–cotton compared to Ag–TiO_2–cotton textiles. Fig. 6a indicates the negligible bacteriostatic action of the cotton textile on *E. coli* in the dark. The cotton sample was subsequently tested under solar simulated light and was able to decrease *E. coli* from 10^6 to 10^3 CFU/ml (Fig. 6b). Fig. 6b reflects the well-known bactericide effect of solar light irradiation on *E. coli* bacteria within 4 h. This result for TiO_2–cotton surfaces differs from the widely reported results for the bactericide action of TiO_2 suspensions under light [14,20]. Fig. 6c shows that the Ag–cotton is so rapid in *E. coli* inactivation, that all bacteria were killed just after contacting with the Ag–cotton surface [21].

The bactericidal activity of the Ag–TiO_2–cotton in the dark is shown in Fig. 6d. It is readily seen that the addition of TiO_2 increases the disinfection time with respect to the Ag–cotton samples. Finally, the Ag–TiO_2–cotton samples used under solar irradiation shown in Fig. 6e lead to an even poorer performance with respect to the same sample tested for its bactericide action in the dark (Fig. 6d). The photochemical reactions induced by TiO_2-light are:

$$TiO_2 \rightarrow e_{cb}^- + h_{vb}^+ \quad (2)$$

$$Ag^+ + e_{cb}^- \rightarrow Ag^0 \quad (3)$$

$$H_2O + 4h_{vb}^+ \rightarrow 4H^+ + O_2 \quad (4)$$

Reaction (3) seems to have taken place in Fig. 6e since the Ag–TiO_2–cotton samples become darker after sunlight irradiation due to the formation of larger Ag-aggregates. The Ag^0 formed would have a lower bactericidal action than Ag^+ present in the Ag–cotton clusters of the Ag–TiO_2–cotton sample in the dark (Fig. 6d) and also in the case of Ag–cotton samples as reported in Fig. 6c. Reaction (3) is possible since the conduction band of TiO_2 (−0.1 V) is more negative than the Ag^+/Ag^0 potential of around 0.70 (V). Ag/TiO_2 has been reported for the case of suspensions enhancing the photocatalytically induced bactericide activity of TiO_2 [22,23] but this is not the case when Ag/TiO_2 is fixed on cotton textiles.

The solid–gas interface of the cotton Ag/TiO_2 allows further reduction of the Ag^+-clusters to Ag^0 on textiles as reported recently by work out of our laboratory [17]. The solid–gas interface has redox properties differ to those found for the solid-aqueous solution interface [22,23]. In both cases, the kinetics, the mechanism and efficiency of the Ag^+ adsorbed into the TiO_2 during the reduction to Ag^0 vary and the silver attains a different degree of reduction in each case. It has been widely reported that for Ag^+-ions deposited on TiO_2, the photo-reductive process leads to the aggregation of silver particles. In Eq. (2), there is a size-dependent redox potential for the reduction of silver-ions that depends on the interfacial processes taking place. These interfacial processes in Eqs. (2–3), determine the aggregation of silver atoms involving electronic and ionic events. Work with suspensions or supported—Ag in the presence of TiO_2 report the initial formation of small homo-dispersed Ag-crystals for both cases [5–8].

4. Conclusions

This study reports the working features for Ag–cotton textiles during the inactivation of *E. coli* in the dark and under light and compares the bactericide performance of this textile with Ag–TiO_2–cotton loaded textiles. Bactericide effects have been evaluated for different samples of Ag-loaded textiles. The Ag–cotton surfaces have been characterized by diverse surface techniques allowing a fair description of the loaded textiles. By depth profile XPS it was possible to assess a penetration of 30 Å for the Ag-clusters in the bleached cotton samples. By TEM, the Ag-cluster size was found for these highly dispersed clusters deposited on the cotton textiles. This study presents the evidence for the detrimental effect of TiO_2 on the Ag-clusters coating cotton during *E. coli* inactivation. The loading of the textile by Ag was determined by elemental analysis and showed that with a very low loading of Ag an efficient bactericide performance was attained. It seems that the efficiency of the Ag^0 dissolution to Ag^+ in the bacterial cell proceeds in a different way in the case of the textile solid-gas interface compared to the case of with Ag–TiO_2 suspensions.

Acknowledgments

This study was supported by the KTI/CTI TOP-NANO21 Program under Grant No. 6117.2 TNS, Bern, Switzerland. We also thank the cooperation of Cilander AG, CH-9100, Herisau, Switzerland.

References

[1] G. Ershov, E. Janata, A. Henglein, J. Phys. Chem. 97 (1993) 339.
[2] F. Fu-Ren, A. Bard, J. Phys. Chem. 106 (2002) 279.
[3] G. Zhao, E. Stevens, Biometals 11 (1998) 27.
[4] C. Tilton, B. Rosenberg, Appl. Environ. Microbiol. (1978) 116.
[5] K. Naoi, Y. Ohko, T. Tatsuma, J. Am. Chem. Soc. 126 (2004) 3664.
[6] J. Kusnetsov, E. Ivanainen, N. Nelomaa, O. Zacheus, P. Martikainen, Water Res. 35 (2001) 4217.

[7] T. Linnert, P. Mulvaney, A. Henglein, H. Weller, J. Am. Chem. Soc. 112 (1990) 4657.
[8] V. Vamathevan, R. Amal, D. Beydoun, G. Low, J. McEvoy, J. Photochem. Photobiol. A 148 (2002) 233.
[9] Q. Feng, J. Wu, G. Chen, F. Cui, T. Kim, J. Kim, Biomed. Mater. Res. 52 (2000) 662.
[10] K. Yoshida, S. Nakamura, M. Naito, T. Yamada, M. Atsuta, J. Dental Res. 79 (2000) 1118.
[11] B. Smith, D. Walters, A. Faulhaber, M. Kreger, T. Roberti, J. Zhang, J. Sol–Gel Technol. 9 (1997) 125.
[12] A. Landsdown, B. Simpson, Br. J. Dermatol. 135 (1997) 728.
[13] German Collection of Microorganisms, DSMZ, Braunschweig, *E. coli* strain K12, Cat. No ATCC 23716.
[14] M. Sokmen, F. Candan, Z. Summer, J. Photochem. Photobiol. A 143 (2001) 221.
[15] E. Szabo-Bardos, H. Czili, A. Horvath, J. Photochem. Photobiol. A 154 (2003) 195.
[16] Y. Yonezawa, N. Kometami, T. Sakue, A. Yano, J. Photochem. Photobiol. A 171 (2004) 1.
[17] T. Yuranova, A.G. Rincon, A. Bozzi, S. Parra, C. Pulgarin, P. Albers, J. Kiwi, J. Photochem. Photobiol. A 161 (2003) 27.
[18] H. Hada, Y. Yonezawa, A. Yoshida, A. Kurakate, J. Phys. Chem. 80 (1976) 2728.
[19] C. Wagner, W. Riggs, L. Davis, J. Moulder, G. Mullenberg (Eds.), Handbook of X-ray Photoelectron Spectroscopy. Perkin-Elmer Corp. Eden Prairie, MN 55344, USA.
[20] A.G. Rincon, C. Pulgarin, Appl. Catal. B 51 (2004) 283.
[21] R. Pedhazur, O. Lev, B. Fattal, H. Shuval, Water Sci. Technol. 31 (1995) 123.
[22] J. Keleher, J. Bashani, N. Heldt, L. Johnson, Y. Li, World J. Microb. Biotech. 18 (2002) 133.
[23] L. Zhang, J. Yu, H. Yip, Q. Li, K. Kwong, A. Xu, P. Wong, Langmuir 19 (2003) 10372.